Gradient Echo Imaging

Michael Markl, Ph.D.
University Hospital Freiburg, Dept. od Diagnostic Radiology,
Medical Physics, Freiburg, Germany

Introduction

Principles and concepts of gradient echo (GRE) imaging are the basis of many applications on modern MR-systems. The most obvious difference between Spin Echo and GRE imaging is related to the pulse sequence elements that are used to generate an MR signal (see figure 1). While two rf-pulses (90^o and 180^o) are used for spin refocusing and spin echo generation, GRE imaging is based on only a single rf-pulse, typically < 90^o, in combination with read gradient reversal. As a result shorter repetition times (*TR*) and therefore faster imaging is feasible. Although signal formation is also more sensitive to field homogeneity and gradient performance, today's advanced hardware permits the successful application of GRE imaging with reliable and reproducible image quality. Many GRE based applications such as dynamic cardiac imaging or MR angiography are an integral part of MR protocols used in routine clinical settings.

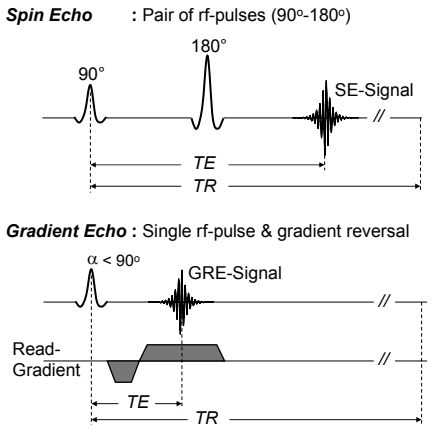

Fig. 1: Simplified spin echo and gradient echo pulse sequence diagrams.

Gradient Echo Formation

In general, any MR signal is created by spin magnetization which is a vector quantity. The magnetization vector can be characterized by its longitudinal component M_z along the direction of the main magnetic field and a transverse component M_{xy} in the plane normal to the main magnetic field. M_z characterizes the magnetization that is available for signal generation which be converted into transverse M_{xy} by rf-excitation with a given flip angle. Once generated, M_{xy} rotates in the transverse plane and induces a detectable MR signal, the so-called Free Induction Decay (FID).
This signal will persist as long as the total magnetization has some component in the transverse plane. However, two relaxation effects (T_1-recovery and T_2*-decay) will affect the amplitude of the signal and result in a fast decay of the signal within milliseconds. T_1-recovery aims at restoring the longitudinal magnetization M_z but, more importantly, local field changes and associated T_2*-effects will result in dephasing of the transverse magnetization and a rapid signal decay on a much shorter time scale.
For a spin echo experiment (figure 2, top) a second 180^o rf-pulse is used to invert the dephasing direction which leads to the formation of a spin echo at echo time *TE* when the dephasing has effectively been reversed. All static field or T_2'-effects, such as susceptibility or field imperfections, are reversed and the signal strength is proportional to T_2 only.

The situation is different for GRE imaging which uses a single rf-pulse in combination with read gradient reversal such that the net gradient area is zero at echo time *TE*. The gradient echo sequence omits the formation of a spin echo and directly uses the signal from the free induction decay following the excitation pulse.

While spin echoes are thus rf-refocused and provide T_2 dependent signal strength, GRE imaging is gradient refocused and has echo amplitudes determined by T_2*-decay.

Mechanisms such as field homogeneity or susceptibility are not refocused at echo time *TE* and will influence the signal and contrast. Note that T_2* includes both T_2 and static T_2'-field effects and is typically much shorter that T_2 alone. As a result, GRE signal intensity decays much faster and echo times have to be shorter as for spin echo imaging on order to yield sufficient signal intensity.

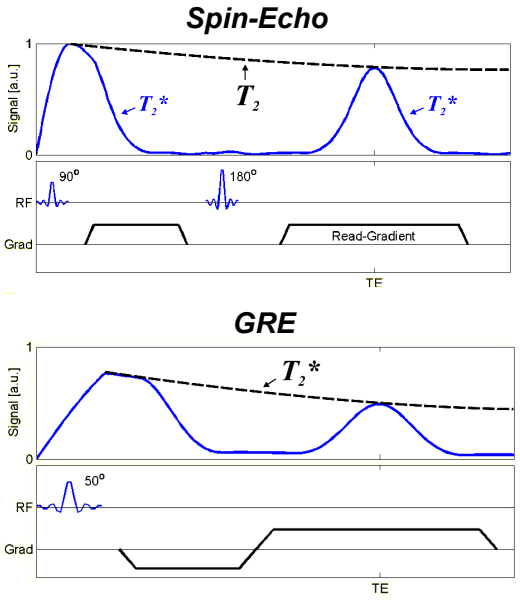

Fig. 2: Signal formation for spin echo and GRE imaging. Note that signal evolution is drawn on different time scales and much shorter echo times are necessary for detectable GRE signal intensity.

SE : Refocused echo ~ T_2
GRE : FID following RF-pulse ~ T_2*

Refocusing: Gradient vs. 180° - pulse
- Corrects only phase shifts from gradient itself
- Other mechanisms …
  - field inhomogeneity, chemical shift, …

… are ***not*** refocused at *TE* as in SE imaging

➔ **GRE signal ~ T_2***

$1/T_2^* = \underbrace{1/T_2}_{\text{Spin-spin effects}} + \underbrace{1/T_2'}_{\text{Inhomogeneity effects}}, \quad T_2^* < T_2$

Basic properties of GRE imaging

Basic GRE Imaging (*TR* >> T_2)

MR imaging typically consists of several repetitions of a basic pulse sequence with given repetition and echo times *TR* and *TE* until all data for a complete 2D or 3D date set are collected. As a consequence, the timing of the acquisition, i.e. *TE* and *TR* relative to signal recovery (T_1) and decay (T_2, T_2*), will determine signal intensity and contrast. In terms of recovery of longitudinal magnetization M_z, gradient echo imaging acts as a pure progressive saturation sequence, such that a so-called steady state will form over several rf-excitations. To illustrate such a steady state formation, figure 3 shows the temporal evolution of the magnetization components M_z and M_{xy} over several pulse sequence repetitions for basic GRE imaging with repetition times *TR* much greater than T_2. Due to the long *TR* the transverse magnetization M_{xy} (dashed lines) completely decays prior to each new rf-excitation. However, since *TR* is typically also much shorter than or of the order of T_1, the longitudinal magnetization (solid lines) will not fully recover to its initial amplitude M_0. Instead, after several repetitions a new equilibrium magnetization M_{SS} is reached. Since the amplitude of each FID is determined by the available longitudinal magnetization M_z that can be converted into transverse magnetization, its new steady state value M_{SS} determines the signal intensity for basic GRE imaging.

In addition, GRE signal intensity depends on the selection of the flip angle. Specifically, signal intensities for a given *TR* and T_1 (i.e. tissue) can be maximized using optimal flip angles, also known as the Ernst angle.

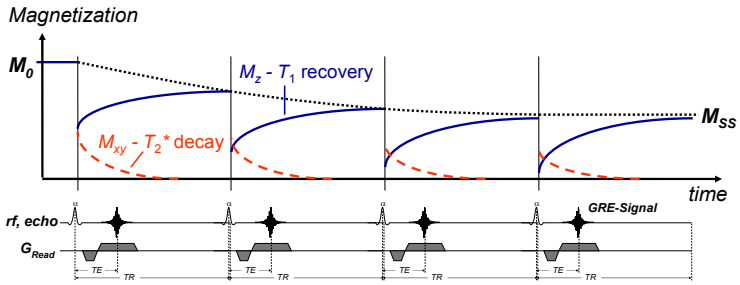

Fig. 3: Steady state formation in basic GRE imaging (*TR* >> T_2).

However, in many imaging applications optimizing the signal from one tissue is not the major concern. More important is optimizing the contrast between two tissues (like lesion and healthy tissue). It has thus to be noted, that even though the signal intensities may be optimal for certain Ernst angles, contrast between tissues with different T_1 is typically maximized at higher flip angles.

Figure 4 summarizes the signal and contrast behavior for basic GRE imaging. Since *TR* is sufficiently long to eliminate any T_2-contributions to the steady state magnetization, images are predominantly T_1-weighted. The highest signal intensities are typically found at low flip angles (between 20° and 40°). Tissue Contrast, however, is optimized for larger flip angles (for example gray and white matter contrast which is maximized between 50° and 60°).

Fast GRE Imaging (*TR* <= T_2)

Fast GRE methods are similar to the previously discussed basic GRE imaging but with short TR and some additional, depending on the specific implementation as spoiled, unbalanced and balanced fast GRE technique.

Since repetition times *TR* are much shorter for fast GRE imaging (<T_2), the transverse magnetization M_{xy} does not fully decay prior to each new rf-pulse and therefore contributes to the steady state formation. In contrast to basic GRE imaging, both the longitudinal (M_z) and the transverse (M_{xy}) magnetization determine the final steady state signal intensity. As for basic GRE, signal intensities demonstrate strong flip angle dependence but more complex contrast, depending on not only on T_1 and *TR* but also T_2.

As a result, unbalanced GRE sequences without any additional modifications (unbalanced GRE) provide high signal to noise (*SNR*) due to coherent use of

Small α	: PD or T_2*contrast (*TE* dependent)
Intermediate α	: T_1-contrast (*TR* dependent)
Large α	: Strong T_1-contrast, low SNR, bright blood

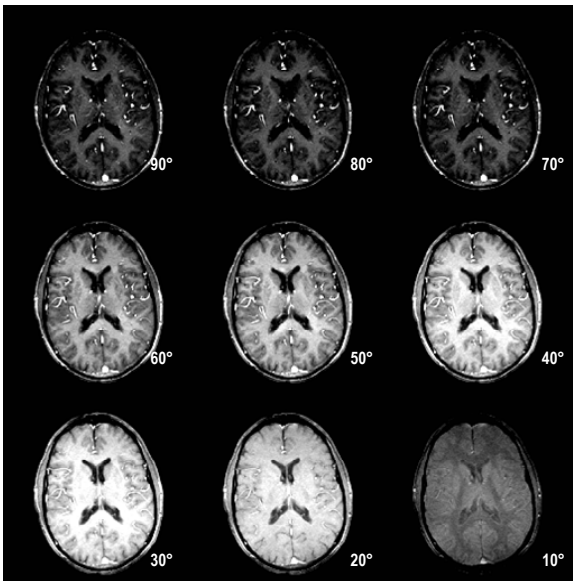

Fig. 4: Signal and contrast or basic GRE imaging as a function of flip angle. Tissue specific optimal signal intensities are achieved using the Ernst angle while contrast is maximized at higher flip angles.

magnetization but offer complex T_2/T_1-contrast that may make image interpretation difficult.

To enhance T_1 contrast while maintaining the short repetition times (*TR*) necessary for fast imaging, a solution is provided by so called spoiling techniques. Gradient spoiling involves additional variable spoiler gradients along the slice and read direction which are varied from one acquisition step to the next. Spins in the transverse plane are deliberately dephased during each *TR* in order to prevent contributions to the GRE signal in subsequent data acquisitions.
A significantly better approach is the so-called rf-spoiling based on incrementing the phase of the rf-pulse from *TR* to *TR*. It can be shown that for certain rf-phase increments the buildup of transverse coherences can be prevented and T_2 contributions can effectively be eliminated.
From figure 5, which shows a side-by-side comparison of a spoiled and a non-spoiled fast GRE acquisition, it is evident that rf-spoiling can successfully be used to eliminate T_2 contributions and enhance T_1 contrast while maintaining short *TR*. It has to be noted, however, that spoiled GRE techniques carry a *SNR* penalty since the transverse magnetization no longer contributes to the total MR-signal. Fast spoiled GRE sequences are used for a wide variety of applications for which the availability of T_1-contrast in combination with short scan times is essential. Important applications include contrast enhanced MR angiography which relies on the T_1 shortening of contrast agents in combination with fast imaging of the passage of an intravenous bolus application (see for example figure 6, normal MRA of the thoracic aorta).

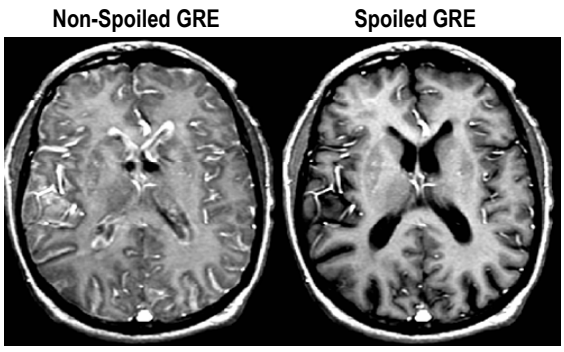

Fig. 5: Comparison of normal and spoiled gradient echo imaging.

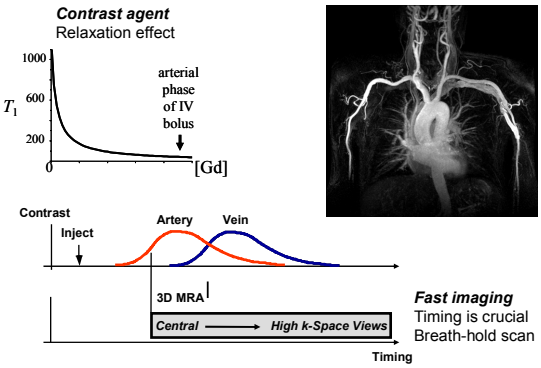

Fig. 6: Contrast enhanced MR angiography. T_1-shortening of intravenously injected contrast agent in combination with appropriate timing of the measurement permits data acquisition of the bolus passage with high arterial signal and contrast.

A third fast GRE variant is known as fully balanced SSFP imaging and has, especially in recent years, gained increased importance in cardiovascular MRI due to its superior signal-to-noise ratio (*SNR*) and in particular blood tissue contrast. Compared to other GRE variants, gradients are fully balanced (i.e. areas vanish over TR), resulting in a more efficient refocusing of the steady state magnetization und thus increased signal. However, balanced SSFP also exhibits a strong sensitivity to local field changes such as local field changes or susceptibility (off-resonance sensitivity).
Signal and contrast for SSFP imaging are a function of the local frequency offset and undergo considerable, local field dependent, changes including areas in which the signal almost completely vanishes (banding artifacts, see figure 7).

In addition to the local field, the repetition time *TR* can substantially influence the SSFP signal. As *TR* is increased, image quality degrades and banding artifacts in areas of high susceptibility become more and more prominent. A combination of good field homogeneity (shim) and short repetitions times is therefore crucial for artifact free SSFP imaging.
SSFP applications are mostly found but not limited to body and cardiovascular MRI. Figure 7 shows results from an ECG gated dynamic studies of cardiac motion in the 4-chamber view. Note the high SNR and also blood tissue contrast of SSFP (bottom row) if compared to rf-spoiled gradient echo imaging (top row).

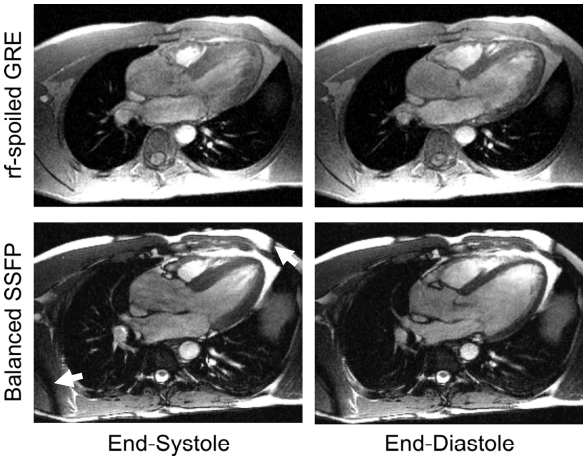

Fig. 7: Time-resolved ventricular performance in a 4-chamber view with balanced SSFP and rf-spoiled GRE. Improved image quality and especially enhanced blood-tissue contrast for balanced SSFP are clearly visible. Note the appearance of SSFP banding artifacts (arrows) visible as signal void in regions of increased field inhomogeneity.

The basic properties of the three most widely used fast GRE techniques are summarized on the right. Unbalanced GRE demonstrates high signal but rather low and complex T_2/T_1-contrast. T_1 contrast is enhanced by the application of rf-spoiling but overall signal intensity is considerable reduced. Balanced SSFP imaging can offer even higher signal but suffers from strong sensitivity to local field changes.

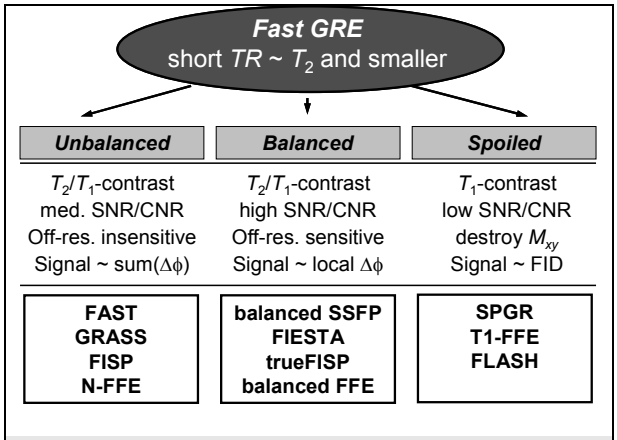

Fast gradient echo imaging variants, basic signal and contrast properties and corresponding vendor specific acronyms.

T_2* and Off-Resonance Effects

One of the fundamental differences between GRE and spin echo imaging is related to the fact that phase shifts from sensitivity to local magnetic field changes, susceptibility etc. are not fully refocused and lead to signal decay governed by T_2*.
For long echo times, signal loss can be severe, as shown by the two GRE images in figure 8 for which longer *TE* leads to an overall decline in signal intensity and almost complete signal dropout in the frontal region with increased susceptibility. For comparison, spin echo imaging (right) is independent of these effects.
However, T_2*-sensitivity of GRE imaging can also be beneficial and used to generate new diagnostic information. For example, T_2*-contrast is used in functional MR imaging (fMRI) where changes in blood oxygenation that lead to alterations in T_2* are used to analyze brain activity. Another widely used application involves the detection of bleeding in stroke patients. Micro-bleeds in such patients lead to local field and therefore T_2*-changes which

can be visualize as signal dropouts using GRE techniques with long echo times. Since such bleedings are very small and hardly detectable with any other imaging modality such the T_2*-GRE imaging is often part of the clinical routine workup of stroke patients.
Additional applications include the analysis of the T_2*-dynamics in contrast agent studies that can be used to generate brain perfusion maps such as regional blow volume and flow.

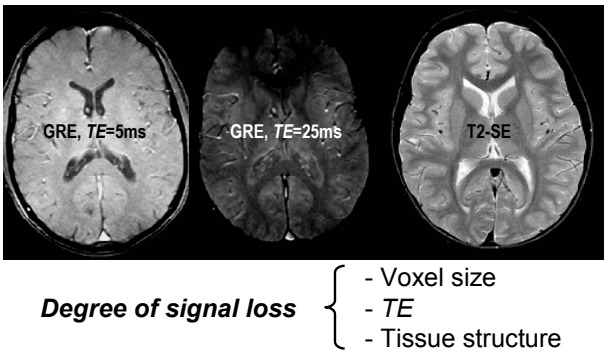

Fig. 8: TE dependence of T_2*-effects in GRE imaging.

A second important T_2*-related effect acting on the observed signal intensity is the chemical shift. Due to the frequency difference of water and fat, their magnetization vectors exhibit a phase difference, which depends on the echo time *TE*. Of special importance are the in-phase (fat and water magnetization are aligned and add) and the out-of-phase (fat and water magnetization are opposed and cancel) conditions. For a 1.5 T magnet images can this be generated that provide contrast generated by opposed (*TE* = 2.2ms, 6.6ms, …) aligned fat water spins (*TE* = 4.4ms, 8.8ms, …).

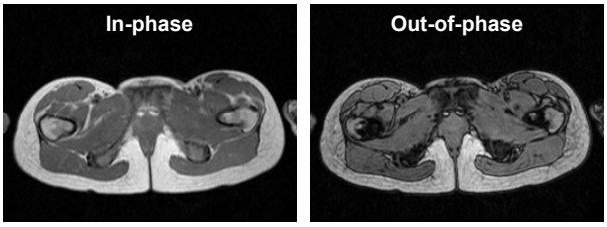

Fig. 9: In-phase and out-of-phase images for GRE imaging with different echo times TE.

Figure 9 shows an example of in-phase/out-of-phase images which can be used to analyze fat and water contents in different tissues. Since fat and water signal add in the in-phase image, signal intensities are typically higher as in the out-of-phase images. Note the occurrence of dark rims at the interface between fatty and aqueous tissues when *TE* is chosen to correspond to the out-of-phase condition. The signal void represents partial volume effects in pixels with roughly equal fat and water contents which cancel and lead to signal void.
Furthermore, the information in both images can be combined and processed for effective fat water separation, e.g. for imaging of joints for cartilage analysis.

Flow Effects

Since signal intensity in GRE imaging is determined by repeated rf-excitation, any static tissue will typically not fully recover prior to the next excitation, resulting in saturated and consequently reduced signal intensities. In contrast, blood that flows into an imaging slice and has not experienced any previous rf-excitations will lead to signal enhancement (bright blood signal).
Such inflow enhancement can be beneficial and used to acquire additional diagnostic information as for example shown in figure 10. Sensitivity to in-flow was used to detect

abnormal venous flow in the left common iliac vein - seen as absent bright venous signal if compared to the right side.
Additional applications include time-of-flight (TOF) techniques in which the in-flow enhancement is used to separate arterial from venous signal in order to generate angiograms.
However, in-flow enhancement can also lead to image artifacts such as ghosting that arises if pulsatile flow leads to amplitude or phase inconsistencies. A solution to this problems is offered by flow compensation techniques which mostly eliminate artifacts but lead to an increase in echo and repetition times *TE* and *TR*.
It should be noted, that flow artifacts can also be minimized by decreasing echo time *TE* such that flow compensation is often obsolete with today's available hardware and imaging parameters

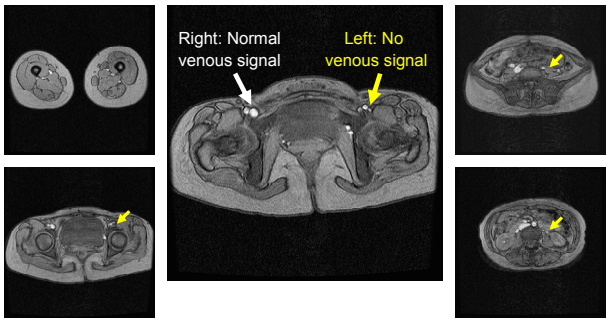

Fig 10: In-flow enhancement and bright blood signal

Magnetization Preparation

In some cases, the intrinsic contrast of GRE imaging techniques may not be sufficient. A potential solution is offered by magnetization preparation techniques which are used to imprint T_1 or T_2 contrast onto the longitudinal magnetization M_z and enhance the desired contrast. A frequently used technique is shown in figure 11 and illustrates enhanced T_1 weighting by inversion recovery imaging. Before the actual start of GRE imaging, an 180° inversion pulse is applied preceding data acquisition by the time-interval or inversion time *TI*. Depending on T_1 of the tissue and the *TI* time, certain T_1 species can be enhanced, suppressed or even nulled.

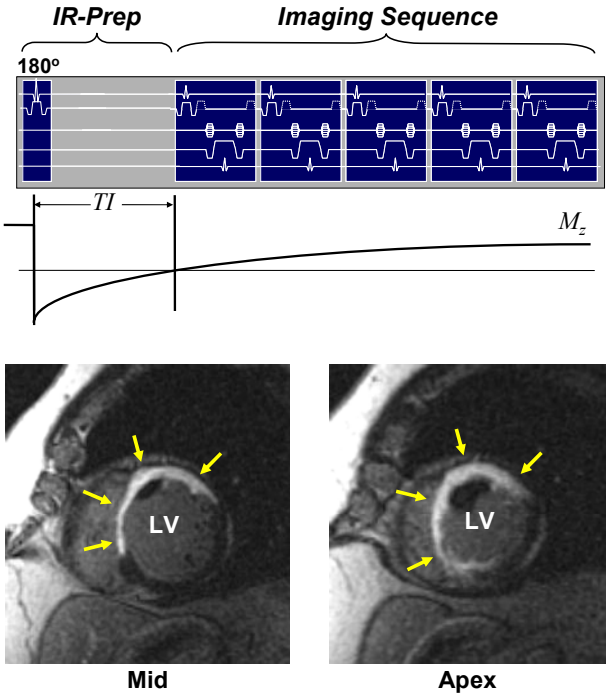

Fig 11: **Top:** Magnetization preparation by inversion recovery for enhanced T_1 contrast. **Bottom:** Delayed hyper-enhancement images of the left ventricle (LV) in a patient with myocardial infarction. Bright areas (arrows) mark regions with irreversibly damaged myocardial tissue.

An inversion recovery application, that has recently gained increased importance, is the 'delayed hyper-enhancement' technique which is used to identify infracted and nonviable tissue in patients with coronary artery disease. Here, the inversion time *TI* is selected such that the myocardial signal is nulled and only contrast agent that accumulates in infracted tissue - and has much shorter T_1 - appears bright in the GRE images (see figure 11).

Summary

The most fundamental difference between GRE and spin echo imaging is related to the fact that echo formation is a result of a single rf-pulse and gradient reversal while spin echo imaging uses a second 180° for echo generation. The signal of a gradient echo sequence is therefore sensitive to various T_2*-effects, which -contrary to spin echo acquisition - are not refocused at the time of signal formation.

SE : Pair of rf-pulses (90°-180°)
GRE : Single rf-pulse (< 90°) & gradient reversal

Fundamental difference:
at *TE*: GRE does *not* refocus phase shifts from
- field inhomogeneity / chemical shift …
➔ T_2*-Effects

Basic GRE, long TR (>T_2)
- Simple T_1-contrast contrast ~ (*TR*, T_1, α)
- T_2* effect for long *TE*
- Strong flip angle dependence - *Ernst Angle*

Fast GRE, short TR (<T_2) :
- Complex contrast ~ (*TR*, T_1, T_2, $\Delta\phi$, α)
- Various methods
- balanced, unbalanced, spoiled

Summary of GRE properties

Signal and contrast for basic GRE imaging (*TR* >> T_2) depend on the formation of a longitudinal steady state. T_2-contribution can be ignored resulting in relatively simple contrast behavior depending on *TR,* T_1 and the flip angel. Of importance are the strong flip angle dependence and existence of optimal flip angles for signal and contrast.

For fast GRE imaging (short *TE* and *TR*), T_2-contribution can no longer be ignored resulting in complex contrast behavior depending on *TR*, T_1, T_2, flip angel and in case of balanced SSFP even local field changes. Fast GRE techniques can be subdivided into unbalanced, balance and rf-spoiled methods. Un-balanced and balanced GRE techniques provide complex T_2/T_1 contrast and high *SNR*. Balanced SSFP offers even higher signal and especially blood tissue CNR but suffers from sensitivity to local field homogeneity. T_1 contrast can be restored by the application of spoiling techniques which offer robust and fast imaging techniques for a variety of applications but suffer from poor *SNR* compared to other GRE variants.

In general, GRE is sensitive to off-resonance effects such as chemical shift or field inhomogeneities which can lead to mis-registration and signal dropout. However, off-resonance sensitivity can also be beneficial and used for perfusion mapping, fMRI, fat water separation and T_2*-contrast. Contrast in 2D GRE imaging is further determined by in-flow enhancement, which can be used to enhance blood tissue contrast as in time-of-flight (TOF) angiography techniques. To enhance T_2- or T_1-contrast magnetization preparation techniques can be combined with GRE imaging.

References

1. Elster AD. Gradient-echo MR imaging: techniques and acronyms. Radiology 1993;186(1):1-8.
2. Sevick RJ, Tsuruda JS, Schmalbrock P. Three-dimensional time-of-flight MR angiography in the evaluation of cerebral aneurysms. J Comput Assist Tomogr 1990;14(6):874-881.
3. Czervionke LF, Daniels DL, Wehrli FW, Mark LP, Hendrix LE., Strandt JA, Williams AL, Haughton VM. Magnetic susceptibility artifacts in gradient-recalled echo MR imaging, Ajnr: American Journal of Neuroradiology 1988;9:1149-1155.

4. Edelman RR, Buxton RB, Brady TJ. Rapid MR imaging. [Review], Magnetic Resonance Annual 1988:189-216.
5. Frahm J, Haase A, Matthaei D. Rapid NMR imaging of dynamic processes using the FLASH technique, Magnetic Resonance in Medicine 1986;3:321-327.
6. Frahm J, Haase A, Matthaei D. Rapid three-dimensional MR imaging using the FLASH technique, Journal of Computer Assisted Tomography 1986;10:363-368.
7. Haacke EM, Tkach JA. Fast MR imaging: techniques and clinical applications. [Review], AJR. American Journal of Roentgenology 1990;155:951-964.
8. Haacke EM, Masaryk TJ, Wielopolski PA, Zypman FR, Tkach JA, Amartur S, Mitchell J, Clampitt M, Paschal C. Optimizing blood vessel contrast in fast three-dimensional MRI, Magnetic Resonance in Medicine 1990;14:202-221.
9. Hawkes RC, Patz S. Rapid Fourier imaging using steady-state free precession, Magnetic Resonance in Medicine 1987;4:9-23.
10. Klose U, Grodd W, Kolbel G. Selective chemical imaging with a three-dimensional gradient echo sequence, Journal of Computer Assisted Tomography 1989;13:724-729.
11. Hennig J. Echoes - How to Generate, Recognize, Use or Avoid Them in MR-Imaging Sequences. Concepts in Magnetic Resonance 1991;3:179-192.
12. Park HW, Kim YH, Cho ZH. Fast gradient-echo chemical-shift imaging, Magnetic Resonance in Medicine 1988;7:340-345.
13. Stadnik TW, Luypaert RR, Neirynck EC, Osteaux M. Optimization of sequence parameters in fast MR imaging of the brain with FLASH, Ajnr: American Journal of Neuroradiology 1989;10:357-362.
14. Haase A, Frahm J, Matthaei K. FLASH Imaging. Rapid NMR Imaging Using Low Flip Angles. Journal of Magnetic Resonance Imaging 1986;67:258-266.
15. Ernst R, Bodenhausen G, Wokaun A. Principles of Nuclear Magnetic Resonance in One and Two Dimensions: Clarendeon Press; 1987.
16. Atkinson DJ, Edelman RR. Cineangiography of the heart in a single breath hold with a segmented turboFLASH sequence. Radiology 1991;178(2):357-360.
17. Zur Y, Wood M, Neuringer L. Spoiling of Transverse Magnatisationin Steady-State Sequences. Magn Reson Med 1991;21:251-263.
18. Haacke M, Brown R, Thompson M, Venkatesan R. Magnetic Resonance Imaging. New York: Wiley-Liss; 1999.
19. Carr HY. Steady-State Free Precession in Nuclear Magnetic Resonance. Physical Review 1958;112(5):1693-1701.
20. Oppelt A, Graumann R, Barfuß H, Fischer H, Hartl W, Schajor W. FISP—a new fast MRI sequence. Electromedica (Engl Ed) 1986;54(54):15-18.
21. Scheffler K, Lehnhardt S. Principles and applications of balanced SSFP techniques. Eur Radiol 2003;13(11):2409-2418.
22. Dumoulin CL, Hart HR, Jr. Magnetic resonance angiography. Radiology 1986;161(3):717-720.
23. Wehrli FW. Time-of-flight effects in MR imaging of flow. Magn Reson Med 1990;14(2):187-193.
24. Siebert JE, Pernicone JR, Potchen EJ. Physical principles and application of magnetic resonance angiography. Semin Ultrasound CT MR 1992;13(4):227-245.
25. Prince MR. Gadolinium-enhanced MR aortography. Radiology 1994;191(1):155-164.